TRIMMING A HIGH-FIDELITY MULTIBODY HELICOPTER MODEL FOR PERFORMANCE AND CONTROL ANALYSIS

Lorenzo Trainelli, Alessandro Croce, Carlo E. D. Riboldi, Radek Possamai
Department of Aerospace Science and Technology, Politecnico di Milano, Milano, Italy

Abstract

This paper brings forward the study of the dynamic behaviour of a novel lightweight helicopter featuring an innovative gimballed two-bladed main rotor. First, previous results for the isolated main rotor are extended for the case of free-coning under cyclic pitch perturbations and longitudinal gusts. Subsequently, the complete helicopter is modelled and a simple control system is derived and applied to steer the helicopter to steady hover and straight flight conditions, showing good characteristics also under gust perturbations.

1. INTRODUCTION

This paper is concerned with the multibody-based modelling of a modern lightweight helicopter currently under development by K4A S.p.A., an Italian rotorcraft manufacturing company (Figure 1), reporting on further steps towards its comprehensive aeromechanical simulation. The vehicle is a two-seat helicopter featuring a two-blade main rotor (MR) and a five-blade tail rotor (TR), both implying highly innovative solutions. In particular, the MR departs from the classical teetering architecture to adopt a complex gimballed rotor head provided with a Bell-Hiller flybar. The gimbal suspension realizes a quasi-constant speed connection between mast and hub, in the quest of significant improvements upon some of the known drawbacks of teetering rotors. These are related to the strong oscillating loads transmitted to the airframe by the MR as a result of hub "wobbling", *i.e.* the typical 2/rev (two per revolution, double the frequency of the rotor) precession motion of suspended 2-blade rotor heads in response to cyclic perturbations. The consequent airframe vibrations significantly impact on vehicle handling qualities, pilot workload, passenger comfort, and structural fatigue.

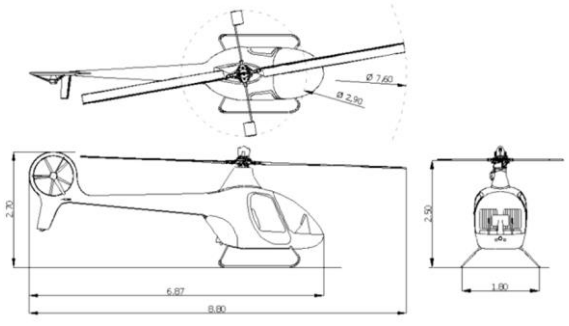

Figure 1. The lightweight helicopter design currently under development by K4A Srl.

Instead of switching towards a multi-blade rotor architecture, an effort intended to preserve the advantages of a two-blade design, in terms of acquisition and operating costs, and ease of stowage and transportation, led Dr. Vladimiro Lidak (1944-2012), a talented Italian rotorcraft designer and inventor, to conceive an innovative homokinetic joint, coupled with a flybar which, on the one hand contributes to the joint actuation at right angles with the blades, while on the other it is integrated in a mixed pitch control mechanism to enhance rotor stability and response characteristics. This represents a fairly original architecture, when contrasted to typical helicopter applications, while being closer to some small remotely-piloted rotorcraft models.

The TR is also based on an original design, being composed by fixed-pitch blades and actuated by a variable-speed motor, in contrast to typical variable-pitch, constant-speed solutions.

The present discussion heavily builds on previously published works.[1,2] In the first reference, the novel MR design and its multibody implementation has been illustrated in detail, together with some studies aimed at determining its peculiar kinematic characteristics and global performance. In the second reference, in-depth studies on the isolated MR dynamic behaviour under cyclic perturbations have been carried out, showing advantages in comparison to classical teetering architectures, as well as sensitivity with respect to various design parameters.

Here, we take some steps forward in two areas:

1. We introduce the MR rotor coning, first as a constant value for both blades and then considering individual blade flapping permitted by a dedicated coning hinge, and study the effects of this additional degree of freedom on the MR dynamic response.

2. We extend the modelling to the complete helicopter, including the TR, as well as the fuselage and fins, in order to develop preliminary trim procedures of the vehicle and appraise some characteristics of the trimmed state.

The result is a highly detailed finite-element multibody model augmented with a control system that steers the system toward a trimmed state. Such a comprehensive model can be useful in various activities such as design verification concerning rotor loads, control authority, and aeroelasticity, as well as comparison with and tuning of a performance model of the aircraft for higher fidelity flight mechanics predictions.

In the following, we briefly describe the multibody implementation of the complete helicopter, referring to previous works for details. Subsequently, we discuss some results concerning the effect of blade coning on the isolated MR response to cyclic perturbations, given by either pitch inputs from the pilot or by longitudinal wind gusts. Next, the proposed trim procedures and some preliminary results for the complete helicopter are shown with respect to hover conditions.

2. MULTIBODY MODEL

2.1. Simulation tool

The complete helicopter model was implemented in the advanced aero-servo-elastic *Cp-Lambda* simulation tool. This is a nonlinear finite-element (FE) multibody code extensively employed in the analysis of rotorcraft and wind-energy industrial systems.[3,4,5,6] *Cp-Lambda* provides a large library of structural elements such as rigid bodies, composite-capable beams and shells, cables, and joint models, which can be equipped with concentrated stiffness and damping, backlash, free-play and friction. Lagrange multipliers enforce the kinematical constraints in an optimized index-3 DAE (differential-algebraic equations) fashion.[7] Among the force fields that can be associated to body elements, aerodynamic forces are modelled according to lifting-line based on 2D aerofoil coefficients. Inflow elements can be associated to rotors, such as the blade-element momentum (BEM) model based on the annular stream-tube theory with wake swirl, or the Peters–He finite-state wake model.[8]

The time integration strategy implemented in *Cp-Lambda* is based on 2nd to 4th order implicit time-stepping schemes characterized by unconditional stability in the full non-linear regime, based on an algorithmic energy decay discretization.[9,10] This unconventional feature reveals highly useful when dealing with complex deformable systems undergoing nonlinear motions. Indeed, FE discretization translates in coupled, numerically stiff systems of equations that yield solutions typically displaying high frequency oscillations. These correspond to poorly resolved spatial scales which significantly impact on the accuracy of the solution, especially in the case when velocity-based force fields are present, such as with aerodynamic forces. Furthermore, high frequency components can be excited as a result of undue energy transfer from lower frequency modes, due to inherent numerical approximations of the time discretization. To overcome these problems, the *Cp-Lambda* solver employs time marching schemes that enforce a tuneable algorithmic energy dissipation, thus providing a built-in filter for unresolved high frequencies. Figure 2 shows the favourable behaviour of the spectral radius and relative period error of this time integrator as functions of the ratio of the time step to the characteristic period of a model linear system.

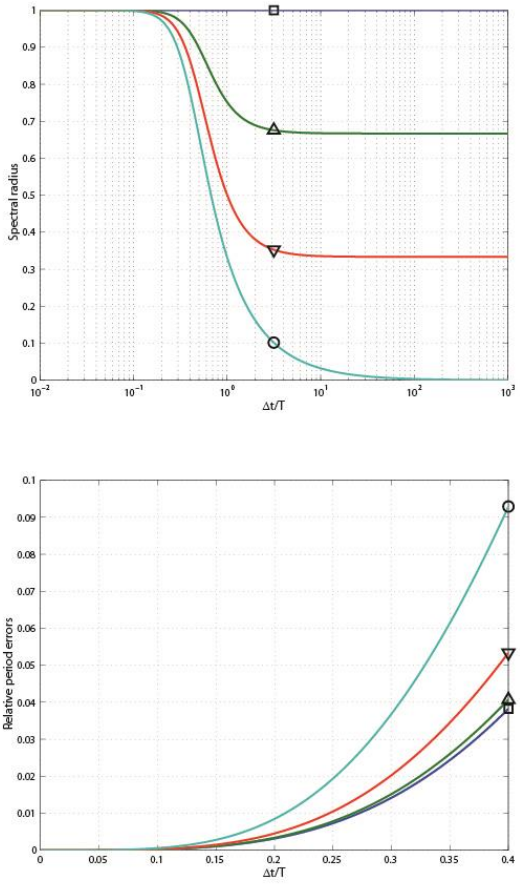

Figure 2. Spectral radius (above) and relative period error (below) of the Cp-Lambda unconditionally stable integrator for different values of the asymptotic spectral radius.

2.2. Main rotor

The MR model includes the complete assembly from the mast and swashplates to the blades. These are represented by geometrically-exact nonlinear beams with associated lifting lines and disk inflow, taking into account twist, sweep and a fully populated stiffness sectional matrix capable of an accurate representation of aeroelastic tailored composite blades. The blades are connected to the hub, which is linked to the mast by way of Lidak's patented constant-speed joint.[11] This gimbal suspension allows the hub to bank freely about two axes normal to the mast, providing a "teetering" movement, *i.e.* a rigid see-saw flapping of the blades, and a "feathering" movement, *i.e.* a tilting of the hub at right angles with the former, roughly corresponding to a blade rotation about their longitudinal axes. The specific mechanical implementation of this joint is fairly complex, compared to standard semi-rigid and articulated rotor heads, and is aimed to provide an adequate approximation of a perfectly homokinetic mast-hub transmission. This consists in an ideal connection ensuring equal values for the mast and hub angular velocities, irrespective of the latter's tilt with respect to the former.

The two hub teetering and feathering degrees of freedom associated with the constant-speed joint are crucial to its behaviour, as, ideally, the elimination of cyclic oscillations in the hub loads would be achieved by restoring local (*i.e.* with respect to hub material axes) vertical flight conditions after a cyclic perturbation. This would be accomplished by the hub tilt in a new banked position, such that no cyclic motions are experienced by the blades with respect to hub material axes. While hub teetering is actuated by the blade cyclic force components, hub feathering relies on the insertion of a flybar of Bell-Hiller type. This element is basically given by a pair of small blades, termed paddles, rigidly fitted to the hub at right angles with the blades. Therefore, the hub feathering motion corresponds to a rigid see-saw flapping of the flybar. As a result, Lidak's peculiar design has proven fairly accurate in approximating an ideal homokinetic joint, as appraised in several kinematic tests, in both two-blade and four-blade rotor applications.[1]

The rotor is stiff-in-plane, since no lead/lag blade motions are permitted, whereas 'coning' hinges are applied at each blade root. Therefore, the blades can flap out-of-plane independently from the hub motion, differently to what previously analysed.[2] This is intended to ameliorate the rotor gust response.

The blades are also connected to the pitch control chain, which transfers the combined effect of a direct (primary) pitch command imposed by the pilot to the swashplate and an indirect (secondary) action generated by hub feathering. This solution is intended to improve rotor stability under gust conditions, by damping the flapping response to cyclic perturbations.

The complex mechanism representing the isolated MR assembly has been faithfully represented by sequences of rigid bodies and lower-pair kinematic joints. Together with the flexible blades, this leads to a system of 59 rigid bodies, 21 beam elements, and 44 mechanical joints totalling 1756 degrees of freedom. This level of fidelity is considered necessary to accurately capture the rotor dynamic behaviour when subjected to a cyclic perturbation from periodic conditions, the so-called wobbling response, and therefore to reliably assess the intensity of oscillating loads transmitted to the fuselage. The reader is addressed to Ref. 1 for the detailed description of the complex mechanisms realizing the gimballed MR head and the mixed pitch control system.

2.3. Airframe and tail rotor

The helicopter airframe basically consists on its fuselage and stabilizing horizontal and vertical fins. These elements are represented by rigid bodies on which aerodynamic forces are applied through appropriate lifting lines.

The TR is represented by a rigid mast/hub assembly to which five beams, representing the blades, are wedged. The blades are rigidly connected to the hub, as no pitch control is required, due to the use of variable-speed actuation. Lifting lines and disk inflow are associated to the TR blades to provide related aerodynamic forces.

Completed with airframe and tail rotor, the comprehensive helicopter multibody model totals over 4200 degrees of freedom, corresponding to 110 rigid bodies, 80 geometrically exact beam elements, and 51 kinematic joints.

3. MAIN ROTOR DYNAMIC RESPONSE

In order to assess the effectiveness of the proposed solution in reducing the amplitude of 2/rev loads transferred to the mast, a number of test simulations have been carried out on the isolated MR. Ref. 2 details a comparative study carried out analysing the dynamic response to cyclic perturbation of four different rotors sharing the same general geometry and the same blades: Lidak's design, its degraded version deprived of pitch mixing, a pure teetering design, and its augmented version endowed with a purely stabilizing flybar (without pitch mixing). In all cases, the models examined do not include the coning hinges and the blades are set normal to the

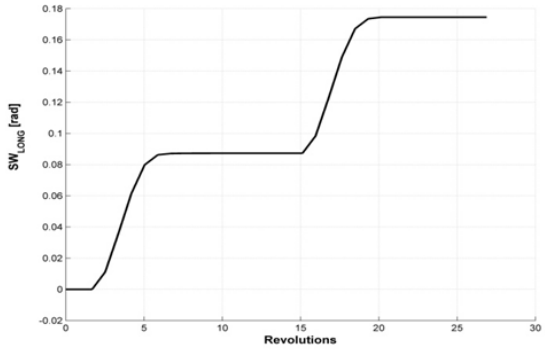

Figure 3. Time history of the primary longitudinal cyclic control input, with two subsequent perturbations of 5° swashplate longitudinal tilt.

hub axis. The results obtained, starting from equal thrust hover conditions, clearly showed a significant superiority of the homokinetic designs, and particularly of Lidak's original design, in terms of hub displacement average values and amplitudes, as well as of force and moment components transmitted by the MR to the mast.

In an attempt to complete the analysis and appraise the effect of MR coning, here we consider first a version of Lidak's rotor with fixed (nonzero) coning, termed $H1_{fixed}$, contrasted to the earlier version with fixed null coning, termed $H1_{flat}$; secondly, we introduce the fully-fledged model with unrestrained individual blade coning, termed $H1_{free}$, to be compared with the $H1_{fixed}$ model. Also, we consider analogous versions of the pure teetering model, termed $T1_{flat}$ and $T1_{free}$. In the fixed (nonzero) coning versions, the cone angle is set to a reference value corresponding to that achieved by the free coning variants at trim.

3.1. Effect of fixed coning

As done in previous work,[2] all models are set in hover conditions at 504 rpm with the application of collective pitch to achieve a thrust value of 9 kN. Upon achievement of the trimmed hover conditions, a cyclic primary control input in the form of a swashplate tilt is applied, quickly rising from zero to 5°, and then to 10° (Figure 3). As a consequence, the rotor leaves its steady-state conditions, tilting towards a wobbling limit cycle. This is a condition in which the hub oscillates twice per revolution about a constant reference orientation, which approximates the ideal tilted configuration. This wobbling motion can be assessed by looking at the hub longitudinal and lateral tilt angles with respect to fuselage-fixed axes, termed u_1 and u_2, respectively.

Figure 4 depicts the wobbling motion of the four models ($H1_{flat}$, $H1_{fixed}$, $T1_{flat}$, $T1_{fixed}$) during the complete transient, until reaching of periodic conditions. Concerning the difference in response

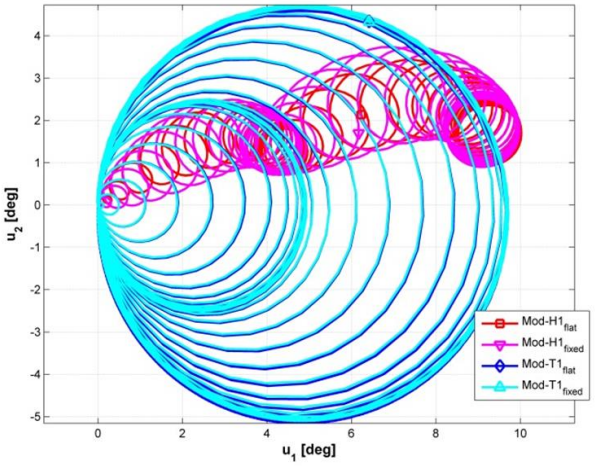

Figure 4. Hub wobbling evolution for the flat models $H1_{flat}$ (red) and $T1_{flat}$ (blue) and the fixed-coned models $H1_{fixed}$ (magenta) and $T1_{fixed}$ (cyan) subjected to two subsequent perturbations of 5° swashplate longitudinal tilt.

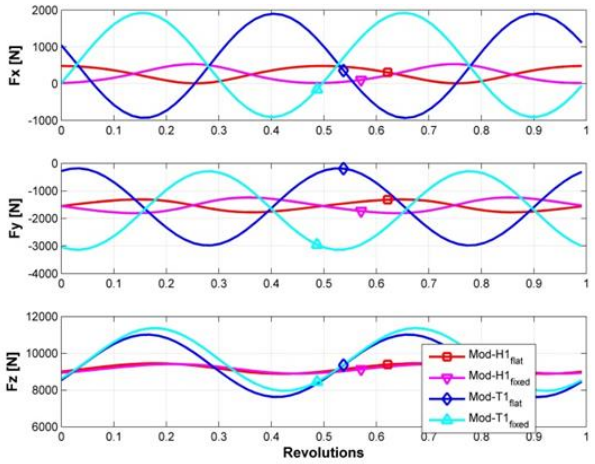

Figure 5. Time histories of the components of the mast internal force for the flat models $H1_{flat}$ (red) and $T1_{flat}$ (blue) and the fixed-coned models $H1_{fixed}$ (magenta) and $T1_{fixed}$ (cyan) in a periodic condition with 10° swashplate longitudinal tilt.

between homokinetic and teetering models, the advantage of the second over the first is fairly evident. In fact, the trend already observed for the $H1_{flat}$ and $T1_{flat}$ models[2] is reproduced here for the $H1_{fixed}$ and $T1_{fixed}$ models. Indeed, while the hub motion for the teetering models describe large circular trajectories passing through the origin (*i.e.* the mast axis), the homokinetic models are characterised by much smaller wobbling oscillations. Furthermore, the average values at periodic conditions for the homokinetic models reach values in the vicinity of u_1 = 10°, which means that the average hub longitudinal tilt is approximately the same as that of the swashplate, with a residual amount of average lateral tilt.

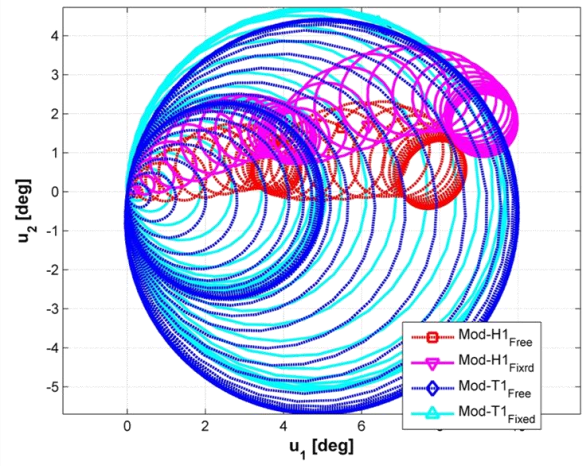

Figure 6. Hub wobbling evolution for the fixed-coned models $H1_{fixed}$ (magenta) and $T1_{fixed}$ (flat) and the free-coned models $H1_{free}$ (red) and $T1_{free}$ (blue) subjected to two subsequent perturbations of 5° swashplate longitudinal tilt.

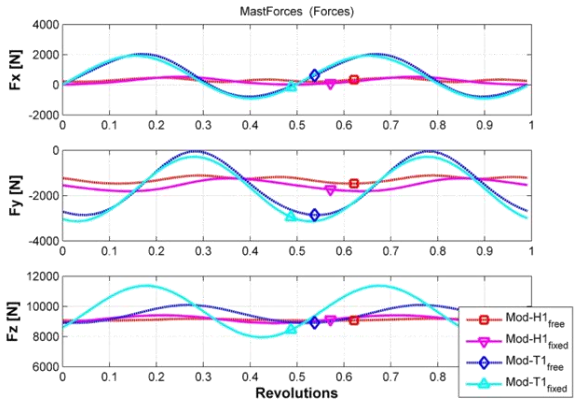

Figure 7. Time histories of the components of the mast internal force for the fixed-coned models $H1_{fixed}$ (magenta) and $T1_{fixed}$ (flat) and the free-coned models $H1_{free}$ (red) and $T1_{free}$ (blue) in a periodic condition with 10° swashplate longitudinal tilt.

Concerning the difference in response with respect to coning value, although slightly better transients can be observed for flat models, the curves do not show a significant impact on steady wobbling average values and amplitudes. This state of affairs is also confirmed by looking at rotor loads transferred to the mast. Figure 5 displays the time histories of the mast internal force components, evaluated with respect to fuselage-fixed axes (*z* being the mast axis) within one revolution in periodic conditions. Again, the wide difference in the amplitude values between the homokinetic and teetering models is apparent, as well as the substantially similar average values and amplitudes. This may suggest that, in the case of simplified analyses using a fixed-coned model, the actual value of the cone angle is not paramount in the evaluation of the wobbling response.

3.2. Effect of free coning

The next analysis considers a comparison between the four models ($H1_{fixed}$, $H1_{free}$, $T1_{fixed}$, $T1_{free}$) in identical conditions as seen above, in order to assess the advantages foreseen for the free-coning models. Figure 6 is analogous to Figure 4 (displaying the same curves for the $H1_{fixed}$ and $T1_{fixed}$ models). Here, a clear disparity appears: while the teetering models exhibit fairly similar behaviour, both during the transient and at periodic conditions, individual blade coning in the homokinetic does not affect amplitudes, but significantly reduces lateral wobbling average values, getting closer to ideal behaviour. Figure 7, analogously to Figure 5, interestingly shows that, while force component and amplitudes at periodic conditions are always smaller for the homokinetic models, there are no significant differences in average values in the case of free coning with respect to fixed coning.

A further step in the evaluation of the effects of free coning is represented by the dynamic response of the homokinetic models ($H1_{fixed}$, $H1_{free}$) as a result of a trapezoidal longitudinal gust from hover linearly rising to μ = 0.1 (V = 20 m/s) and subsequently linearly vanishing (μ represents the rotor advance ratio, *i.e.* airspeed divided by the blade tip rotational speed). Figure 8 shows the resulting hub wobbling, which drifts relatively regularly towards periodic conditions when maximum advance ratio is achieved, before returning to the initial state when the gust is over. We note that the (nonlinear) response of both models under rising and declining relative wind conditions are not superposed. Here again, free coning reduces the average values of the hub oscillations, and also slightly damps the amplitudes, both during the transients and at periodic conditions. This effect is magnified when

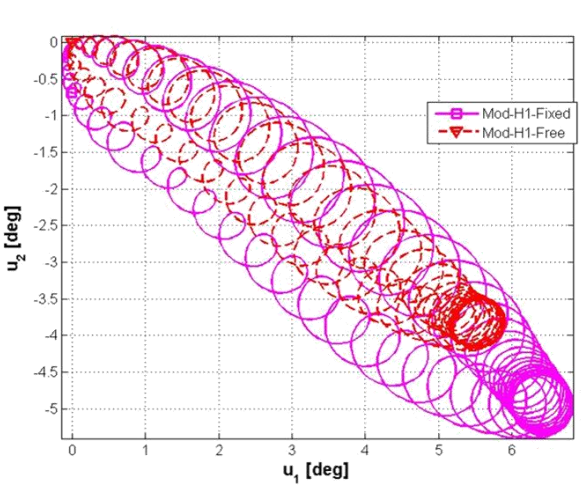

Figure 8. Hub wobbling evolution for the free-coned models $H1_{fixed}$ (magenta) and $H1_{free}$ (red) subjected to a trapezoidal gust reaching μ = 0.1 from hover.

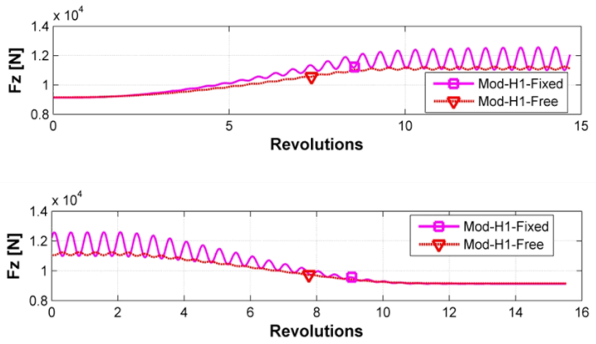

Figure 9. Time history of the mast axial force for the free-coned models $H1_{fixed}$ (magenta) and $H1_{free}$ (red) subjected to a trapezoidal gust. Above: transition from hover to μ = 0.1. Below: transition from μ = 0.1 to hover.

looking at mast loads. In fact, the effects of the transitions from hover to steady relative wind and back to hover on the mast axial force (related to thrust oscillations) displayed in Figure 9 indicate a remarkable reduction in both average values and amplitudes for the free-coned model, to the advantage of handling qualities, fuselage vibratory conditions, and structural fatigue.

4. COMPLETE HELICOPTER TRIM

4.1. General considerations

Helicopter trim conditions can be broadly defined as those in which the fuselage maintains a steady state, *i.e.* constant linear and angular velocities with respect to body-axes, with constant control inputs. This corresponds to a periodic motion of the main rotor.[12] Such a condition is computed with relative ease using performance models, such as those based on Prouty's formulation,[13] which adopt drastic simplifications in the MR representation. However, such ad-hoc approaches allow to capture the global flight mechanics behaviour, but lack the ability to determine the full nonlinear dynamic behaviour of the main force generator aboard the vehicle, the MR, and thus are inherently unfit to capture significant aeroelastic features such as rotor blade deformations, loads and vibrations. Trimming a high-fidelity, fully nonlinear model poses more difficulties, given the complexity of the unsteady motion of virtually all elements within each single revolution.

In addition, given the nature of the swashplate-actuated pilot pitch control, a constant cyclic input do not translate in perfectly 1/rev periodic MR rotor loads, as higher harmonic components are triggered by rotorcraft aerodynamics. Furthermore, the typical helicopter in hover and low-speed rectilinear flight conditions displays inherent dynamic instability, along with significant coupling about its fuselage

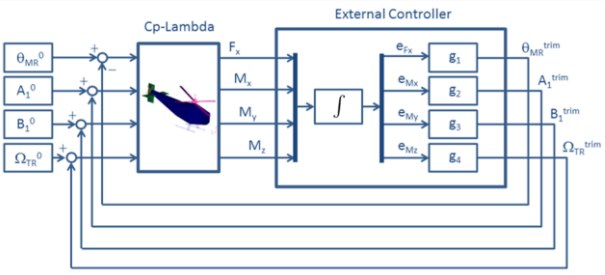

Figure 10. Functional scheme of the preliminary trim approach based on the ground-constrained helicopter.

body axes.[14] This practically translates, in the necessity of a continuous, time-varying application of cyclic control by the pilot, the so-called "stick stirring", to achieve a (quasi-)steady hover or low-speed straight flight conditions. Therefore, an averaged notion of constant instantaneous motion for the fuselage must be considered.

In order to steer the multibody model of the complete helicopter, integrating the $H1_{free}$ MR, to achieve and maintain trimmed conditions, a closed-loop control system has been designed and coupled with the *Cp-Lambda* code. This system is basically an autopilot that actuates the four helicopter controls, *i.e.* MR collective pitch θ_0, MR lateral and longitudinal cyclic pitches A_1 and B_1 and TR rotational speed N_{TR}, to achieve arbitrary trimmed flight conditions at given values of helicopter gross weight, airspeed and altitude. The control system architecture is fairly simple, presenting four PI (proportional + integral) channels, one for each control separately, closing the loop on four separate helicopter states. Indeed, given the inherent dynamic coupling of helicopters, this elementary implementation does not deal with cross-coupled responses in an optimized way. Nonetheless, it has been chosen because its basic implementation is straightforward and relatively inexpensive, while retaining acceptable performance in steering the complex multibody model to quasi-steady conditions. The control system development involved two steps, with different philosophies.

4.2. Preliminary application to the constrained helicopter

We devised first an approach for a fast assessment of trimmed hover conditions by constraining the helicopter model to the ground through a dedicated beam element, and applying a control strategy based on force and moment feedback. This implies that the control system seeks equilibrium conditions attempting to annihilate the loads transferred by the helicopter to the ground, using the constraining beam and a load cell sensor. In particular, the autopilot actuates the MR collective pitch θ_0 (the main responsible for thrust generation) to achieve a

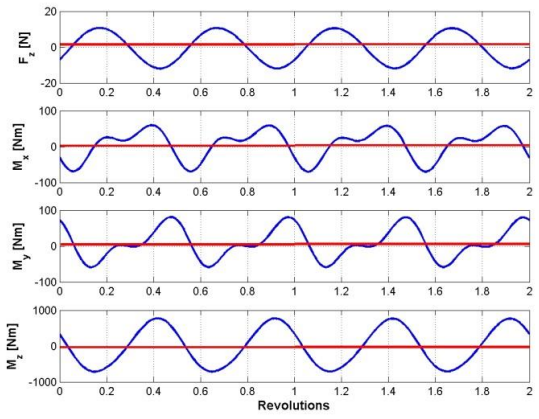

Figure 11. Time histories of the components of the ground-transferred vertical force, roll moment, pitch moment and yaw moment in a quasi-hover condition

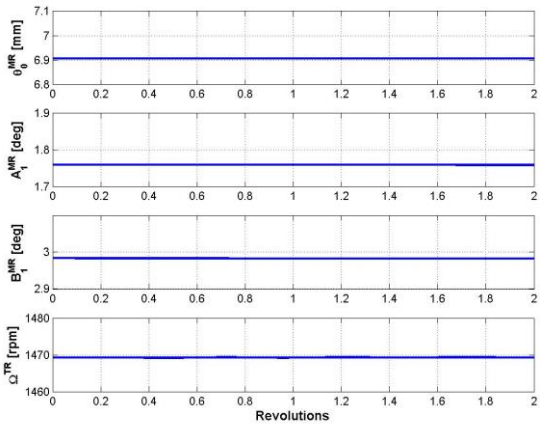

Figure 12. Time histories of the collective pitch, lateral cyclic pitch, longitudinal cyclic pitch and tail rotor speed in a quasi-hover condition for the constrained helicopter.

null vertical force F_z set point, the MR lateral and longitudinal cyclic pitches A_1 and B_1 (charged with the thrust tilting with respect to the mast) to achieve null rolling and pitching moments M_x and M_y, and TR control N_{TR} (principal enforcer of the fuselage directional attitude) to annihilate the yawing moment M_z. Figure 10 shows the functional scheme of this preliminary approach.

Examples of the results of this process are given in Figures 11 and 12, displaying load components and control inputs, respectively, in a hovering case. It appears that loads oscillate about null average values, confirming the achievement of a quasi-trimmed condition. The amplitudes of such oscillations are very small, save for a non-negligible value of the yawing moment, considered acceptable in view of the limited capabilities of the control scheme to dominate the inherent lateral/directional coupling. Looking at flight controls, it is noted that MR quantities are essentially constant, while the TR control basically oscillates about a constant value.

In order to appraise the quality of this solution, the ground constraint was removed and the uncontrolled free-flying helicopter model was actuated with constant control values obtained as the average of the actual time functions obtained at trim. The inevitably unstable open-loop response is depicted in Figures 13 and 14, The first presents the time histories of the helicopter centre-of-mass displacement components, while the second gives the components of the Wiener-Milenkovic (CRV) rotation vector[15] representing fuselage attitude. A slow drift without oscillations is obtained for all quantities, which will eventually lead to an unlimited motion evolution. This, in the present setting, appears an acceptable estimation for the actual free-

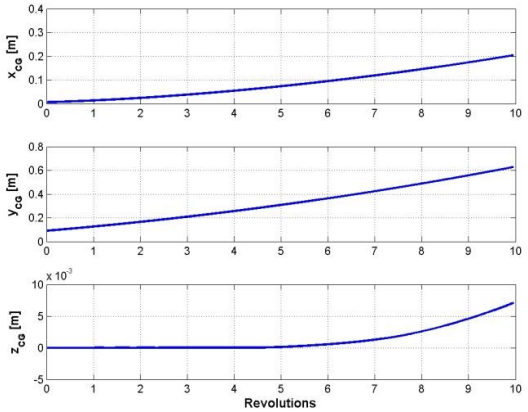

Figure 13. Time histories of the components of the helicopter centre of mass displacement in an open-loop quasi-hover condition for the free-flying helicopter.

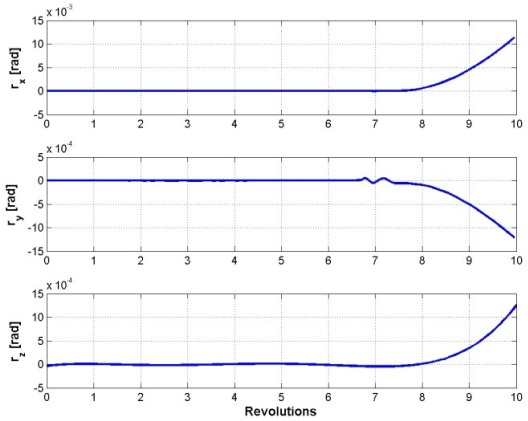

Figure 14. Time histories of the components of the fuselage Wiener-Milenkovic (CRV) vector in an open-loop quasi-hover condition for the free-flying helicopter.

flight trimmed conditions, since the 'gentle' drift does not entail any significant short-term effect on the global vehicle response, nor on rotor dynamics.

The obtained trim solution is clearly characterised by non-vanishing lateral and longitudinal cyclic pitch values, due to the need of contrasting the TR thrust and accommodate the weight moment at the hub centre due to the centre of mass position away from the mast axis. Therefore, it is interesting to assess if the imposition of these 'correct' trim controls to the isolated MR makes any difference in its perturbative response compared to the previously considered 'collective-only' steady conditions. Figure 15 compares the u_1 and u_2 responses to the trapezoidal longitudinal gust seen before for the isolated rotor, starting either from the simplified steady conditions already considered, or from the pitch controls corresponding to the complete helicopter trimmed hover, which produce a constant wobbling. It appears that wobbling perturbations from initial steady-state conditions are almost the same for the two cases, as confirmed by taking the difference between the envelopes of the corresponding curves. Therefore, we conclude that complete initial conditions including cyclic pitch controls seem inessential on the global perturbative behaviour, and that pure collective application appears sufficient for assessing the isolated rotor response to cyclic perturbations.

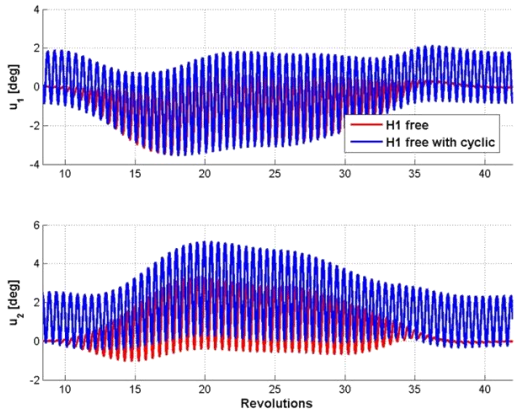

Figure 15. Time histories of the longitudinal and lateral hub tilt angles for the isolated $H1_{free}$ rotor model subjected to a trapezoidal gust reaching μ = 0.1 from hover: 'collective-only' initial conditions (red) vs. 'collective & cyclic' initial conditions retrieved from complete helicopter trim (blue).

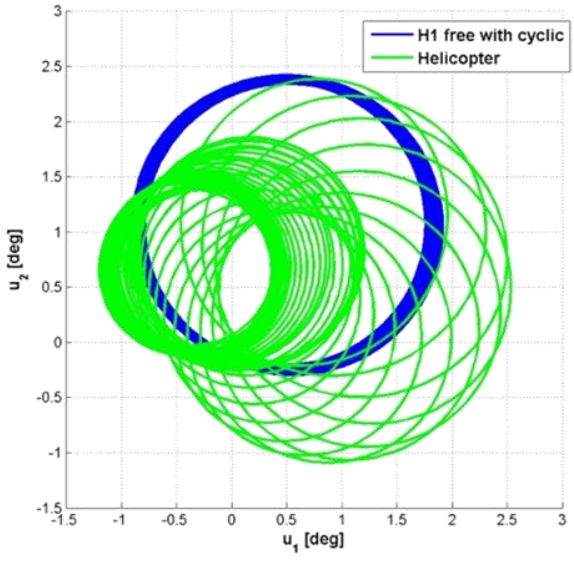

Figure 16. Hub wobbling evolution for the isolated rotor (blue) and the complete helicopter rotor (green) subjected to a doublet gust reaching V = ±0.5 m/s from hover.

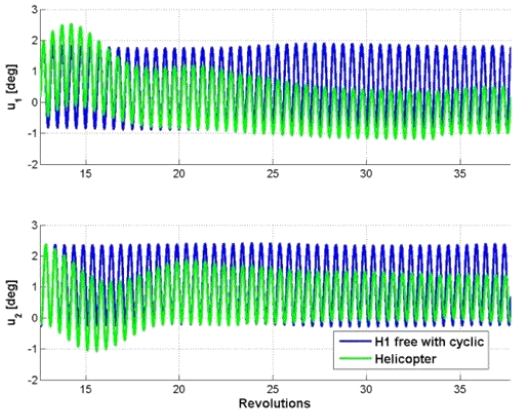

Figure 17. Time histories of the longitudinal and lateral hub tilt angles for the isolated rotor (blue) and the complete helicopter rotor (green) subjected to a doublet gust reaching V = ±0.5 m/s from hover.

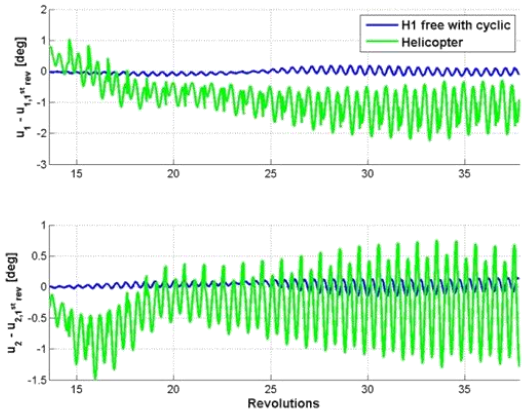

Figure 18. Time histories of the perturbations in longitudinal and lateral hub tilt angles for the isolated rotor (blue) and the complete helicopter rotor (green) subjected to a doublet gust reaching V = ±0.5 m/s from hover.

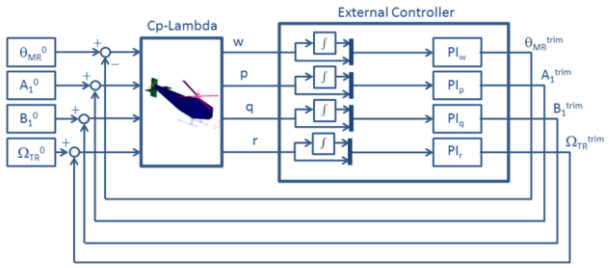

Figure 19. Functional scheme of the proposed trim approach for the free-flying helicopter.

On the other hand, the open-loop response of the free-flying helicopter MR deeply differs from that of the isolated rotor, even considering complete initial conditions. Figure 16 shows the u_1 and u_2 response of the two systems perturbed from hover by a longitudinal gust in the form of a doublet with V = 0.5 m/s (μ = 0.0025) peak values. As apparent, the isolated rotor is only slightly affected by this weak disturbance, while the helicopter MR, in absence of feedback control, is driven to a banked periodic condition when the transient is over. Figure 17 shows that the complete helicopter rotor globally experiences lower wobbling amplitudes, but looking at the perturbations form the initial state, *i.e.* the differences between the values attained at each rotor revolution and those attained in the first revolution, the situation is opposite. Figure 18 demonstrates that these perturbations are much higher for the uncontrolled complete helicopter rotor, which inevitably displays a highly sensitive behaviour.

4.3. Application to a free-flying helicopter

In order to obtain a more general and flexible trim procedure, building on the previous simple control scheme, another autopilot has been designed to steer a free-flying helicopter to a given equilibrium condition. This control system attempts to annihilate the difference of the components of fuselage rigid motion in body axes with respect to a reference set point. In particular, this autopilot actuates the MR collective pitch θ_0 to achieve a given value of the vertical velocity w, the MR lateral and longitudinal cyclic pitches A_1 and B_1 to achieve given values of the roll and pitch rates p and q, and TR control N_{TR} to achieve a given value of the yaw rate r. Figure 19 shows the functional scheme of this preliminary approach.

As a first result of this improved control approach, we appraise the quality of a trimmed hover solution by looking at the values retrieved for the controls and for the displacement of the helicopter centre of mass, shown in Figures 20 and 21, respectively. It can be seen that the controls at trim are characterised by negligible oscillations,

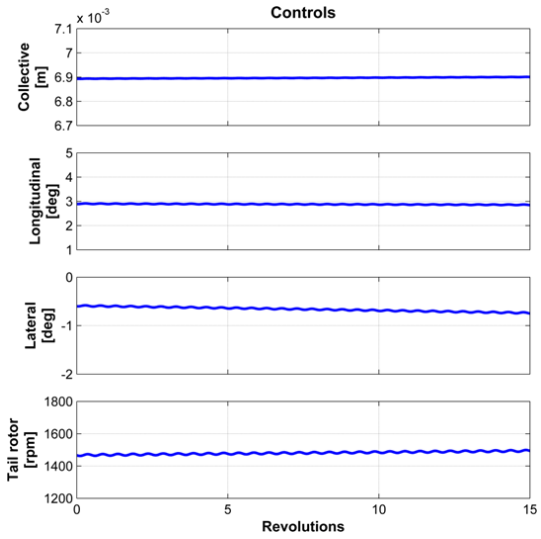

Figure 20. Time histories of the flight controls in a hover condition for the free-flying helicopter.

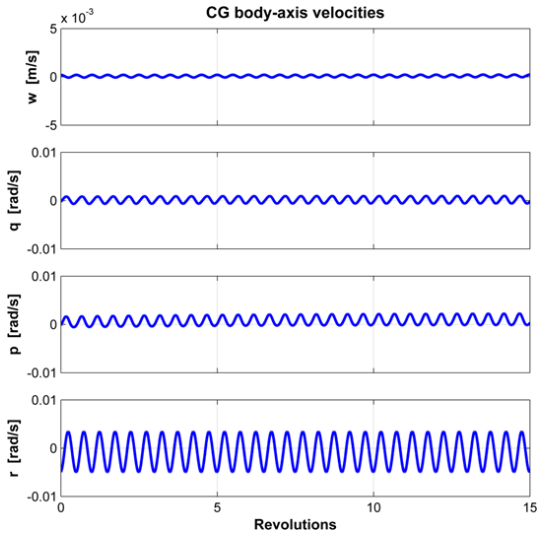

Figure 21. Time histories of the body-axes vertical speed and angular rates in a hover condition for the free-flying helicopter.

corresponding to "stick stirring", about sensibly constant values (at least in a short-term evaluation, as a slight drift is observed for the cyclic pitches and the tail rotor control). Correspondingly, the controlled variables (w, p, q, r) appear fairly well tracked, again with negligible superposed oscillations.

On the score of these promising results, the controlled helicopter in hover has been subjected to a trapezoidal longitudinal gust with 5 m/s peak value, to assess the ability of the autopilot to compensate the perturbations and steer the vehicle back to hover conditions. Figure 22 shows the time histories of the gust profile, the flight controls, and the controlled kinematic variables in this case. As apparent, the control system effectively negotiates the relative wind perturbation, without introducing

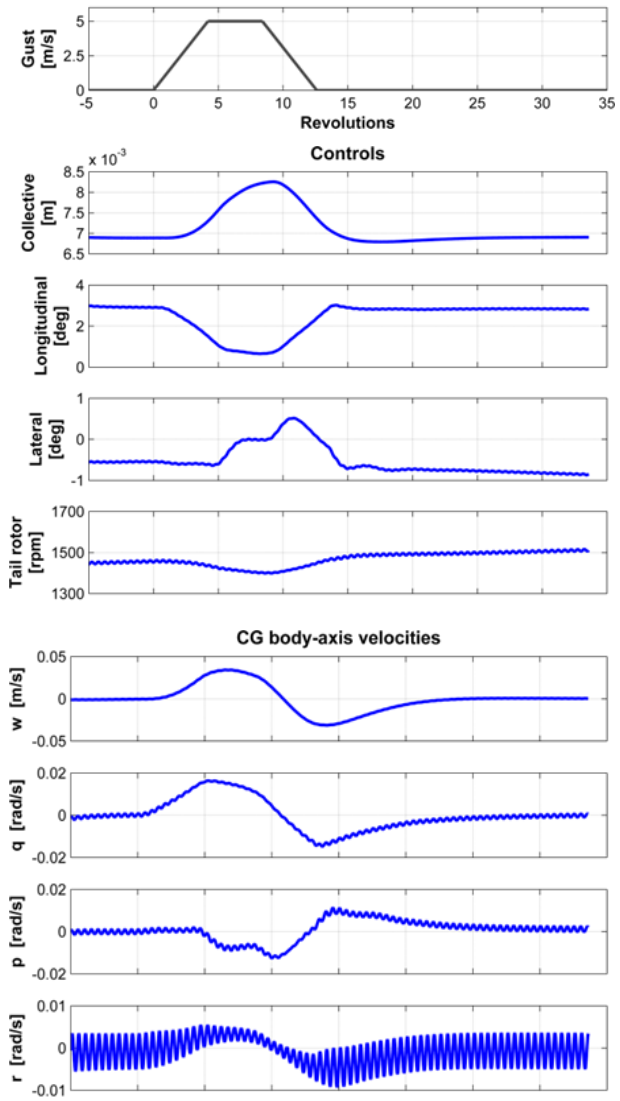

Figure 22. Time histories of the trapezoidal longitudinal gust, the flight controls and the body-axes vertical speed and angular rates for the free-flying helicopter perturbed from hover conditions.

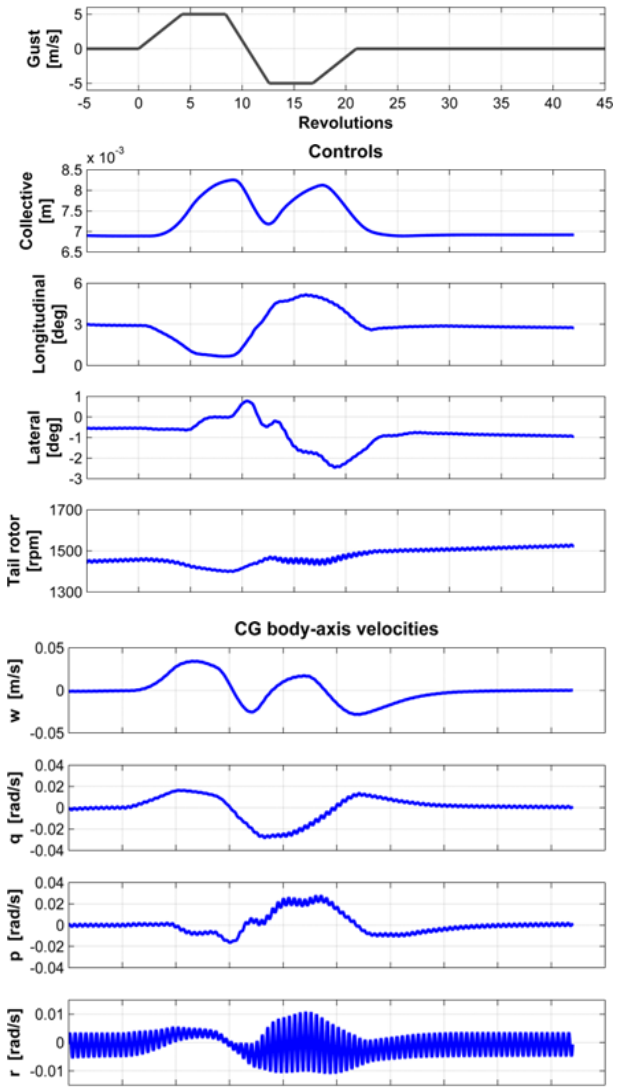

Figure 23. Time histories of the longitudinal gust doublet, the flight controls and the body-axes vertical speed and angular rates for the free-flying helicopter perturbed from hover conditions.

any undue oscillation and effectively leading the helicopter to unperturbed conditions. The limitations due to the simplicity of the uncoupled PI control strategy do not seem to harm the closed-loop behaviour of this complex rotorcraft system. This is confirmed by a second simulation in which the initially hovering helicopter is hit by a longitudinal gust doublet with ±5 m/s peak values, as seen in Figure 23.

Finally, an example of a trimmed forward flight condition is presented. Here, the helicopter is steered to a steady horizontal flight at an airspeed of 10 m/s (μ = 0.05). In this case, the same control system employed for hover has been applied, without modifications. Figures 24 and 25 illustrate the values retrieved for the controls and for the displacement of the helicopter centre of mass, respectively. It can be seen that the forward flight condition, although no changes were applied to the controller PI gains, appears characterised by an analogous quality, with fairly regular controls and a slightly higher oscillatory behaviour for the controlled variables (w, p, q, r), globally very close to their common null set point. Figure 26, articulated along the same pattern as Figures 22 and 23 show the time evolution of relative wind intensity, flight controls and controlled kinematic variables for a doublet gust perturbation applied on the helicopter trimmed in forward flight. Again, the previous considerations on the control system aptitude apply to this low speed flight condition.

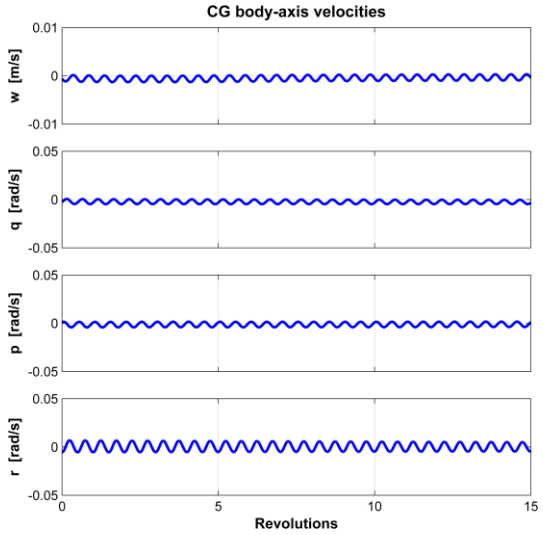

Figure 24. Time histories of the body-axes vertical speed and angular rates in a 10 m/s forward flight condition for the free-flying helicopter.

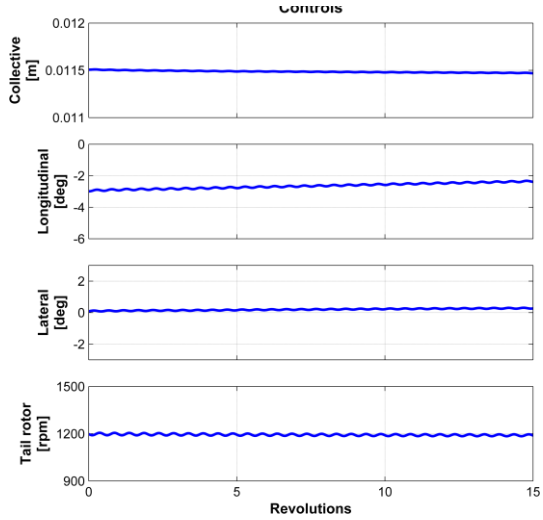

Figure 25. Time histories of the flight controls in a 10 m/s forward flight condition for the free-flying helicopter.

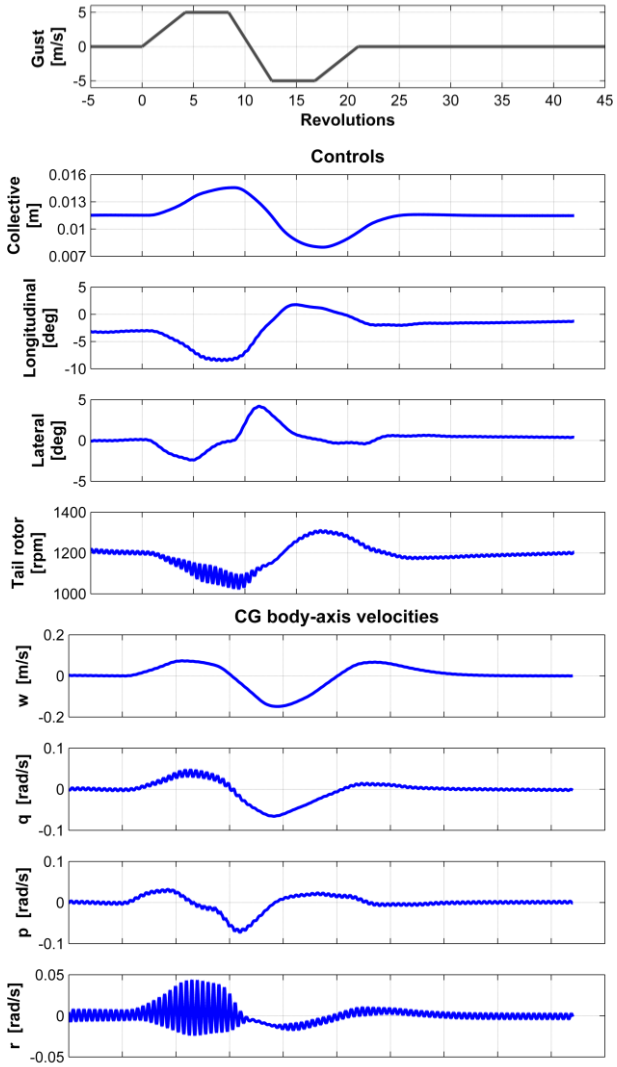

Figure 26. Time histories of the trapezoidal longitudinal gust, the flight controls and the body-axes vertical speed and angular rates for the free-flying helicopter perturbed from 10 m/s forward flight conditions.

5. CONCLUSIONS

The present contribution continues the study undertaken in previous works,[1,2] aiming at the characterisation of the dynamic behaviour of a novel lightweight helicopter equipped with an innovative two-bladed gimballed main rotor. The peculiar characteristics of this rotor require a highly detailed numerical model, which proves able to capture its nonlinear wobbling response, proving the superiority of this design compared to traditional teetering rotors. The simulations carried out in this work confirm the foreseen advantages in providing the rotor with free individual blade coning hinges, allowing the blades to flap independently from the hub motion, which significantly reduces oscillatory motions caused by impinging gusts.

The extensive studies performed on the isolated main rotor constitute a solid base to engage the study of the dynamics of the complete helicopter. To this end, the numerical model has been completed with the fuselage, fins and tail rotor and a simple autopilot based on a four-channel uncoupled PI control strategy has been derived in order to steer the vehicle model to achieve steady state hover or rectilinear flight conditions. This procedure, although liable to be further refined, yields satisfactory results, trimming the vehicle in spite of the strong coupling about all axes and the system inherent dynamic instability. It has also been shown that the autopilot successfully takes on gust perturbations from trim

conditions, insuring smooth transients with limited, low-frequency oscillations and an effective return to unperturbed conditions.

This simulation set up is currently applied to a wider range of flight conditions, aiming to compare the trim parameters (*e.g.* the flight control values, the vehicle attitude, the aerodynamic angles of the fuselage and the main rotor) with those obtained by a lower fidelity, relatively inexpensive performance model. This will allow to identify the modelling capabilities and limitations of such an approach for the specific application at hand, and to correct the performance model to better fit the higher-fidelity results. In addition, the developed model can be used to retrieve useful information concerning control authority, rotor loads, and broadly speaking the vehicle aeroelastic behaviour and its sensitivity to changes in design parameters.

Future lines of action currently being considered also include the refinement of the control system, possibly changing strategy from PI to a model-based approach, in an attempt to derive a general purpose, flexible tool to perform response and stability analyses in arbitrary points of the helicopter's flight envelope, including sizing manoeuvres and off-design conditions.

ACKNOWLEDGEMENTS

The authors gratefully acknowledge the collaboration of graduate students Andrea Castagnoli and Carlo Capocchiano.

REFERENCES

[1] Croce A, Possamai R, Savorani A, Trainelli L. Modelling and Characterization of a Novel Gimbal Two-Blade Helicopter Rotor. Proc. 40th European Rotorcraft Forum (ERF2014), Southampton, UK, paper no. 079, 2014.

[2] Croce A, Possamai R, Trainelli L. Dynamic Properties of Some Gimbal and Teetering Two-Blade Helicopter Rotor Heads. Proc. 40th European Rotorcraft Forum (ERF2014), Southampton, UK, paper no. 080, 2014.

[3] Bottasso CL, Trainelli L, Abdel-Nour P, Labò G. Tilt Rotor Analysis and Design Using Finite-Element Multibody Dynamics Proc. 28th European Rotorcraft Forum (ERF 2002), Bristol, UK, 2002.

[4] Bottasso CL, Croce A, Leonello D, Riviello L. Steering of Flexible Multibody Models with Application to the Simulation of Maneuvering Flight. Proc. 4th European Congress on Computational Methods in Applied Sciences and Engineering (ECCOMAS 2004), Jyväskylä, Finland, 2004.

[5] Bottasso CL, Riviello L. Trim of rotorcraft multibody models using a neural-augmented model-predictive auto-pilot. *Multibody System Dynamics*, Vol. 18, No. 3, pp 299–321, 2007.

[6] Bottasso CL, Croce A, Savini B, Sirchi W, Trainelli L. Aeroelastic Modeling and Control of Wind Turbine Generators Using Finite Element Multibody Procedures. *Multibody System Dynamics*, Vol. 16, No. 3, pp. 291–308, 2006.

[7] Bottasso CL, Dopico D, Trainelli L. On the Optimal Scaling of Index Three DAEs in Multibody Dynamics. *Multibody System Dynamics*, Vol. 19, No. 1/2, pp. 3–20, 2008.

[8] Peters DA, He CJ. Finite state induced flow models. Part II: Three-dimensional rotor disk. *Journal of Aircraft*, Vol. 32, pp. 323–333, 1995.

[9] Bottasso CL, Borri M, Trainelli L. Integration of Elastic Multibody Systems by Invariant Conserving/Dissipating Algorithms – Part II: Numerical Schemes and Applications. *Computer Methods in Applied Mechanics and Engineering*, Vol. 190, No. 29/30, pp. 3701–3733, 2001.

[10] Bauchau OA, Bottasso CL, Trainelli L. Robust Integration Schemes for Flexible Multibody Systems. *Computer Methods in Applied Mechanics and Engineering*, Vol. 192, No. 3/4, pp. 395–420, 2003.

[11] Lidak V. Constant Velocity Joint for helicopter rotors. Patent WO/2010/128378/A2, 2010.

[12] Peters DA, Barwey D. A General Theory of Rotorcraft Trim. *Mathematical Problems in Engineering*, Vol. 2, No. 1, pp. 1–34, 1996.

[13] Prouty RW. *Helicopter Performance, Stability, and Control*. PWS engineering, Boston, 1986.

[14] Johnson W. *Helicopter aeromechanics*. Cambridge University Press, Cambridge, 2013.

[15] Bauchau OA, Trainelli L. The Vectorial Parameterization of Rotation. *Nonlinear Dynamics*, Vol. 32, No. 1, pp. 71–92, 2003.